Polymer 53 (2012) 316–323

Contents lists available at SciVerse ScienceDirect

Polymer

journal homepage: www.elsevier.com/locate/polymer

Thermoresponsive graphene nanosheets by functionalization with polymer brushes

Jae Min Bak [a,1], Taemin Lee [b,1], Eunyong Seo [b], Youngil Lee [a], Han Mo Jeong [a], Byeong-Su Kim [b,**], Hyung-il Lee [a,*]

[a] Department of Chemistry, University of Ulsan, Ulsan 680-749, Republic of Korea
[b] Interdisciplinary School of Green Energy and School of NanoBioscience and Chemical Engineering, UNIST (Ulsan National Institute of Science and Technology), Ulsan 689-798, Republic of Korea

ARTICLE INFO

Article history:
Received 22 September 2011
Received in revised form
22 November 2011
Accepted 26 November 2011
Available online 3 December 2011

Keywords:
Thermoresponsive polymer brushes
FGSs
PDMAEMA

ABSTRACT

We report the preparation of thermoresponsive graphene nanosheets functionalized by the polymer brushes. This approach involves the direct growth of thermoresponsive polymer brushes from functional graphene sheets (FGSs) by chemical modification with initiators followed by extension with poly(2-(dimethylamino)ethyl methacrylate) (PDMAEMA) through surface-initiated atom transfer radical polymerization. The highly controllable polymerization method affords the hybrid FGS-PDMAEMA with tailorable length of PDMAEMA brushes possessing the average molecular weight (M_n) ranging from 7.4×10^3 to 6.0×10^4 with low molecular weight distributions ($M_w/M_n = 1.09$ −1.22). The resulting FGS-PDMAEMA was carefully characterized with a number of techniques, including elemental analysis, thermogravimetric analysis, differential scanning calorimetry, X-ray photoelectron spectroscopy, scanning electron microscopy, and transmission electron microscopy, all supporting the successful integration of polymer brushes onto the surface of FGS. Most importantly, we accomplished the reversible phase transfer of this hybrid FGS-PDMAEMA between aqueous and organic phases via temperature control by taking advantage of the thermoresponsive nature of PDMAEMA brushes. Moreover, the composite film prepared by depositing the suspensions of FGS-PDMAEMA demonstrated the facile control over the wettability upon temperature changes. This tailored control over dispersion in water, selective solubilization between aqueous and organic solvents, and wettability control upon temperature variation have a significant impact on the ability to improve properties of hybrid graphene-based materials. Because of the highly versatile and tunable properties of surface-initiated atom transfer polymerization, we anticipate that the general concept presented here offers a unique potential platform for integrating responsive polymers for graphene nanosheets for advanced electronic, energy, and sensor applications.

1. Introduction

Graphene, a monolayer of aromatic carbon lattices, has drawn considerable attention from many fields of science and engineering in recent years with its extraordinary electrical, thermal, and mechanical properties [1–3]. While earlier synthetic methods for graphene were challenging, there have been considerable advancements in synthesis and processing methods, such as micromechanical exfoliation [4], chemical oxidation/reduction protocols [5–7], epitaxial growth [8,9], and chemical vapor deposition [10–12], which bring graphene into the realm of current nanotechnology. Among various types of graphene and its related carbon nanostructures, functionalized graphene sheets (FGSs) [13–15] are considered, particularly, to be the most common choice over pristine graphene owing to its facile synthetic nature in a controlled, scalable, and reproducible manner from a natural graphite. Indeed, taking full advantage of the versatile chemical modification methods on the graphene nanosheet, together with its unique physical and mechanical characteristics, graphene nanosheets are promising for the creation of functional hybrid nanomaterials with various polymers [16,17]. Recent progress in integrating graphene nanosheets into the polymer matrix include simple solution mixing [18,19], melt compounding [20,21],

* Corresponding author.
** Corresponding author.
E-mail address: sims0904@ulsan.ac.kr (H.-i. Lee).
[1] These authors contributed equally to this work.

0032-3861/$ – see front matter © 2011 Elsevier Ltd. All rights reserved.
doi:10.1016/j.polymer.2011.11.057

non-covalent stabilization [22,23], in situ polymerization [24,25], covalent attachment of preformed polymers [26], and direct polymerization from the graphene surface [27–31].

In realization of the hybrid graphene-polymer nanocomposites [32,33], fine control over the chemical compositions, structures, and stabilizing the interface between the graphene nanosheets and polymers are key factors to synergistically translate the characteristics of each component to the resulting hybrid nanomaterials. In that regard, achieving a stable dispersion of graphene-polymer nanocomposites in a wide range of dispersion media continues to be a challenging endeavor for the fabrication of smart graphene-polymer nanocomposite materials.

Polymer brushes are assemblies of polymer chains which are attached on a surface. Even though they can be anchored to the surface by physical attraction, covalent attachment is often preferred since this method can improve the miscibility between the substrate and polymer chains. In general, two approaches are employed to prepare polymer brushes: 'grafting-to' [34] and 'grafting-from'. The grafting density of polymer brushes prepared by the "grafting-to" method is usually low due to steric congestion between the substrate and the pre-synthesized polymer chains with functional end groups. On the other hand, densely-grafted polymer brushes can be readily produced by the "grafting-from" method through surface-initiated polymerization [35].

The conformation and physical properties of the macromolecules are influenced by various stimuli such as temperature, pH, and light [36]. Among those, thermoresponsive polymers which exhibit a lower critical solution temperature (LCST) undergo phase separation upon heating above their LCST. In aqueous solutions, these polymers are soluble below the LCST through hydrogen bonding with water molecules but become insoluble upon heating above the LCST. When thermoresponsive polymers are combined with FGSs, it is expected that the dispersion state of FGSs can be reversibly controlled by temperature, which is applicable for the area of graphene-based switching devices and sensors.

With the combination of the unique features of graphene and thermoresponsive polymer, poly(2-(dimethylamino)ethyl methacrylate) (PDMAEMA) brush, herein, we present the reversible phase transfer of graphene sheets between aqueous and organic solvents upon temperature changes. For that purpose, we introduced thermoresponsive polymer brushes onto the surface of graphene nanosheets via surface-initiated atom transfer radical polymerization (SI-ATRP) [37–39]. This method enables the facile control over the degree of polymerization and affords the necessary stability of the resulting hybrid graphene-polymer nanocomposite in a wide range of solvents. Though there are recent examples of growing polymeric brushes on top of graphene sheet [27,40–42], this report is unique in that we have utilized the thermoresponsive property of the polymer brushes particularly in tailoring the dispersibility of graphene sheet as well as the wettability of graphene thin films. The successful dispersion of graphene sheets is anticipated to enable the use of low-cost solution processing techniques to fabricate graphene-based materials and further broaden their application in relevant technological areas.

2. Experimental

2.1. Materials

Functional graphene sheets (FGS) were prepared using the Brodie method. 2,2-(dimethylamino)ethyl methacrylate (98%, DMAEMA) was purified by passing through a column filled with basic alumina to remove inhibitors. CuBr (98%), ethyl α-bromoisobutyrate (EBiB, 98%), 4-aminophenylethyl alcohol (98%), isopentyl nitrite (96%), α-bromoisobutyryl bromide (98%), trifluoroacetic acid (99%) were purchased from Aldrich and used as received. *N*,*N*,*N*′,*N*″,*N*″-pentamethyldiethylenetriamine (PMDETA) was purchased from Tokyo Chemical Industry (TCI) and used as received.

2.2. Synthesis of polymer brush on FGS

2.2.1. 4-hydroxylethylphenyl FGSs (FGS-OH)

FGSs (1.00 g, 10 mmol), 4-aminophenethyl alcohol (13.72 g, 100 mmol), isopentyl nitrite (150 mL, 1.11 mol) were added to a 500 mL three-neck round-bottom flask equipped with a stir bar and condenser. The reaction flask was sealed with a septum. The flask was filled with nitrogen, heated in an oil bath at 60 °C, and refluxed for 3 h. The reaction mixture was filtered over a filter paper (pore size; 5 mm, Advantec), washed with acetone (300 mL), DMF (300 mL), and acetone (300 mL). This process was repeated several times until the impurities were completely removed. Finally, the mixture was washed with a diethyl ether (300 mL) and dried overnight in a vacuum oven at 60 °C to give 4-hydroxylethylphenyl FGSs (FGS-OH, 2.20 g).

2.2.2. 2-bromo-2-methylpropanoate-4-methylphenethyl FGSs (FGS-Br)

FGS-OH (2.20 g, 22 mmol) was added to a 500 mL round-bottom flask and dispersed in dry THF (50 mL) by sonication for 30 min. To this triethylamine (61.31 mL, 440 mmol) was added, followed by the dropwise addition of α-bromoisobutyryl bromide (54.38 mL, 440 mmol) in ice bath for 2 h. The mixture was allowed to stir for 48 h at room temperature. The reaction mixture was filtered over a filter paper (pore size; 5 m, Advantec), washed with acetone (300 mL), THF (300 mL), DMF (300 mL), and distilled water (300 mL). This process was repeated several times until the impurities were completely removed. Finally, the product was washed with a diethyl ether (300 mL) and dried overnight in a vacuum oven at 60 °C to give 2-bromo-2-methylpropanoate-4-methylphenethyl FGSs (FGS-Br, 2.54 g).

2.3. FGS-PDMAEMA

A clean and dry Schlenk flask was charged with FGS-Br (0.10 g), DMAEMA (15.3 mL, 90 mmol), PMDETA (31.5 μL, 0.15 mmol), anisole (15.3 mL), EBiB (44 μL, 0.30 mmol). The flask was deoxygenated by five freeze-pump-thaw cycles. CuBr (21.45 mg, 0.15 mmol) was added to the frozen mixture in the atmosphere of argon. The flask was heated in an oil bath at 50 °C. After predetermined time-point, the mixture was periodically taken out from a Schlenk flask to determine the monomer conversion and molecular weight. The polymerization was finally stopped at 16 h by exposing the mixture to air. FGS-PDMAEMA was purified using Soxhlet extraction in acetone to remove free polymers which could be physically adhered to the surface of FGS-PDMAEMA. The resulting FGS-PDMAEMA was dried under vacuum at room temperature for 24 h (1 h; M_n = 11,700 g/mol, M_w/M_n = 1.07), (2 h; M_n = 17,300 g/mol, M_w/M_n = 1.06), (3 h; M_n = 22,000 g/mol, M_w/M_n = 1.08), (4 h; M_n = 26,700 g/mol, M_w/M_n = 1.09), (5 h; M_n = 30,700 g/mol, M_w/M_n = 1.10), (16 h; M_n = 58,200 g/mol, M_w/M_n = 1.22).

2.4. Characterizations

The apparent molecular weights and molecular weight distributions were measured by GPC (Agilent technologies 1200 series) using a polystyrene standard with DMF as the eluent at 30 °C and a flow rate of 1.00 mL/min. Surface morphology of the samples was investigated using scanning electron microscopy (SEM, FEI, NOVA NANOSEM 230) and energy-filtering transmission electron microscope (TEM, Carl Zeiss-LIBRA 120). Surface functional groups of

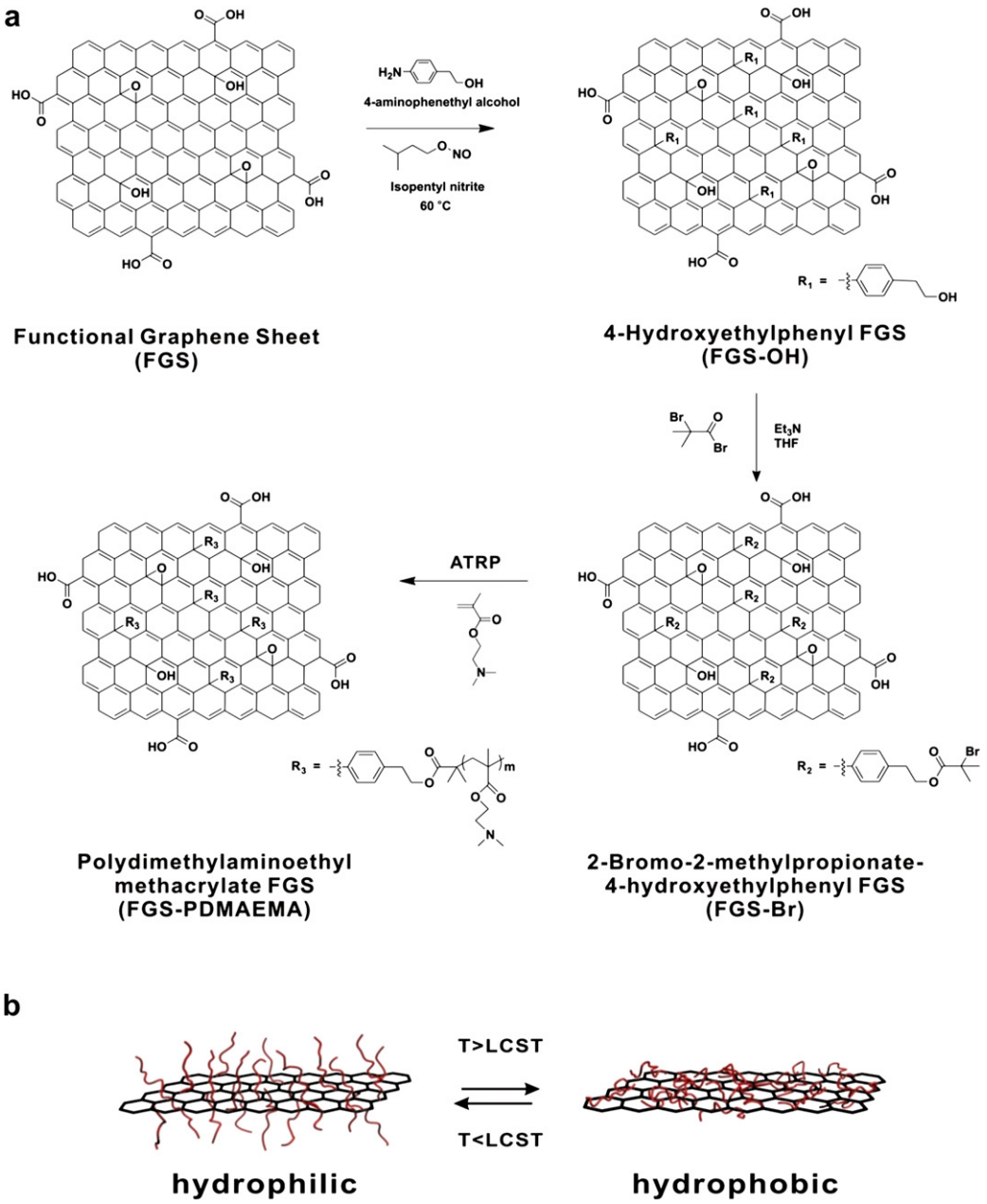

Scheme 1. (a) Schematic illustration of the synthetic process for the FGS-PDMAEMA brushes grown from the surface of FGS via SI-ATRP. (b) The thermoresponsive LCST behavior of FGS-PDMAEMA.

FGS-PDMAEMA were characterized by XPS (Thermo Fisher, K-alpha). The composition of each component within the FGS-PDMAEMA was measured by using thermogravimetric analyzer (TGA, TA Instrument). Element analyzer (Thermo Scientific) determined the weight percentages of carbon, hydrogen, nitrogen, and oxygen of the FGS-PDMAEMA with varying degree of polymerizations.

3. Results and discussion

Graphite oxide (GO) was prepared using the modified Brodie method from a commercially available graphite powder. It is generally believed that each layer of GO consists of randomly distributed non-oxidized aromatic regions and aliphatic regions with polar groups, such as hydroxyl, epoxide, ether, and carboxylate groups, originated from oxidation [43]. Functionalized graphene sheets in bulk quantities were produced through thermal reduction of GO. When a sufficiently oxidized GO is heated in an inert environment over 1000 °C, it can be exfoliated into a few layered graphene sheets, affording the functionalized graphene sheets (FGSs). The treatment of FGSs with 4-aminophenethyl alcohol in the presence of isopentyl nitrite resulted in diazonium salts with hydroxyl groups (FGS-OH). The ATRP initiator on the surface of FGSs (FGS-Br) was then introduced by esterification between FGS-OH and α-bromoisobutyryl bromide. In this approach, diazonium addition involves direct functionalization of sp^2 carbons of FGSs, which enables high loading of ATRP initiating groups on the surface. As a result, even though thermal and

electrical properties are slightly decreased, polymer brushes with high grafting density can be synthesized, which leads to excellent water dispersibility and film properties. Water-dispersible 'hairy' FGS-polymer hybrids were prepared by grafting PDMAEMA from FGS-Br by surface-initiated ATRP (SI-ATRP), as illustrated in Scheme 1. A CuBr/PMDETA catalyst system was employed for the SI-ATRP of DMAEMA using ethyl 2-bromoisobutyrate (EBiB) as a sacrificial initiator to control chain propagation on the surface as well as to determine monomer conversion and molecular weight. It is generally believed that the free polymer initiated by the sacrificial initiator in solution has almost identical molecular weights to those formed from the solid support. A small amount of the samples were taken by syringe at regularly spaced intervals in order to monitor conversion and evolution of the molecular weight. The molecular weight (M_n) and molecular weight distribution (M_w/M_n) of the soluble PDMAEMA formed from a sacrificial initiator were obtained using a gel permeation chromatography (GPC) with polystyrene (PS) standards. As shown in Fig. 1, the GPC traces with monomodal distributions shifted continuously toward higher molecular weight throughout the polymerization while the molecular weight distribution was relatively low, indicating good control over the grafting polymerization, at least for chains growing freely in solution. For FGS-PDMAEMA-16 h, the apparent molecular weight (59,200 g/mol) of all samples obtained by GPC was higher than the theoretical molecular weight calculated from the HEMA conversion ($M_{n,\text{theory}}$ = conversion × MW_{DMAEMA} × $[DMAEMA]_0/[EBiB]_0$ = 0.35 × 157 g/mol × 600 = 32,970 g/mol) due to the differences in hydrodynamic volumes of PHEMA and PS standards as well as the high population of terminated polymers by coupling reaction in solution. The ATRP of DMAEMA from FGS-Br yielded well-defined hybrid materials, judging from the controlled molecular weight and low polydispersity of the polymers isolated from solution.

Thermogravimetric analysis (TGA) was employed to access the relative composition of polymers within the FGS-PDMAEMA composite and its thermal stabilities. For clear comparison, pristine FGS, and surface-initiator modified FGS-Br were identically subjected to TGA at a heating rate of 10 °C/min under N_2 environment (Fig. 2). As shown in the TGA curve, the FGS shows a mass loss of 28% upon heating to 1000 °C, which is attributed to the oxygen-containing functional groups contained in the surface of the FGS. Upon functionalization with the surface-initiator for ATRP, the FGS-Br exhibited an initial mass loss of about 15% at 235 °C due to the cleavage of the initiator moiety, and followed by a final mass loss about 44%. The successful functionalization of the initiator moiety is further corroborated by the elemental analysis which reveals the presence of ca. 12% of Br in the FGS-Br (Table 1). In addition, the controlled nature of ATRP was clearly demonstrated in the TGA

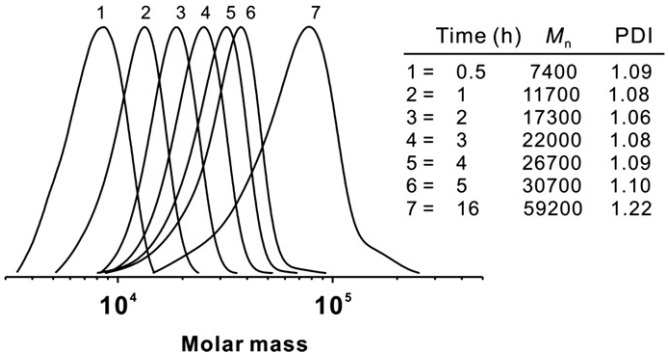

Fig. 1. GPC traces for the series of PDMAEMA with different polymerization time. The GPC traces were collected from the PDMAEMA using a sacrificial initiator, EBiB, in DMF with PS standards.

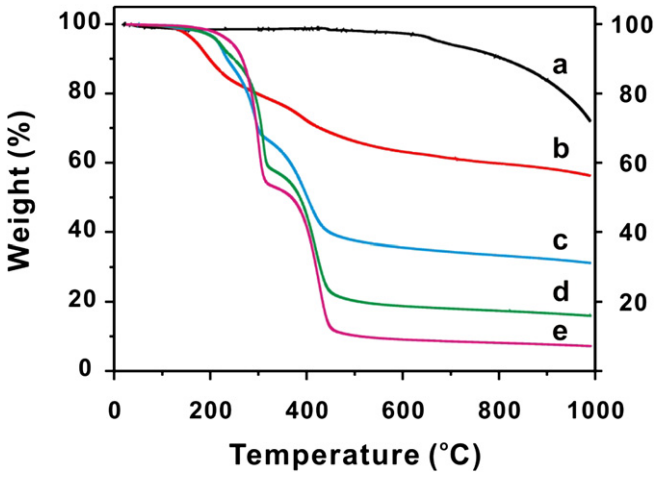

Fig. 2. TGA thermograms of (a) FGS, (b) FGS-Br, and (c–e) FGS-PDMAEMA samples with different polymerization time: (c) FGS-PDMAEMA-1 h, (d) FGS-PDMAEMA-3 h, (e) FGS-PDMAEMA-16 h. The thermograms were obtained with a heating rate of 10 °C/min in N_2.

curve, which indicated that the different polymerization time influenced the degree of polymerization within the FGS-PDMAEMA, which in turn displays the differences in the relative composition of PDMAEMA in FGS-PDMAEMA composites. For example, the FGS-PDMAEMA samples with 1, 3, 16 h polymerization time showed the 68.9%, 84.1%, and 92.8% of decomposition relative to starting materials of FGS-Br (44.0% degradation), respectively, which indicated a relative composition of 24.9%, 40.1%, and 48.8% of PDMAEMA brushes were grafted onto the surface of FGS. While TGA data are a little inconsistent with the apparent molar mass of the polymers measured by GPC, they matched well with the theoretical molar mass of the polymers measured by monomer conversion. It is also of note that all the FGS-PDMAEMA composite exhibited a sharp mass loss in the range of 250–400 °C, resulting from the decomposition of PDMAEMA, and followed by the gradual evolution of labile surface functional groups on the FGS. Independent to the TGA results, an elemental analysis determined the elemental weight fraction of C, H, N, O of FGS-PDMAEMA-16 h to be 63.71%, 8.45%, 7.88%, and 19.96%, respectively (average of 3 different batches) (Table 1). Based on the changes in the nitrogen content, we can calculate approximately 30% of PDMAEMA was present in the hybrid FGS-PDMAEMA composite, which is comparable to that observed with TGA. Provided that all grafted initiators initiate the polymerization, the amount of PDMAEMA grafted to graphene nanosheets was evaluated to be 32,970 g/mol, which is slightly higher than that of linear chains produced during polymerization process.

We have also investigated the differential scanning calorimetry (DSC) of the FGS-PDMAEMA, however, we could observe a subtle 0.7 °C difference of the glass transition temperature (T_g) of the PDMAEMA with respect to that of free polymer with a similar

Table 1
Elemental analysis of the samples prepared in this study[a].

Entries	C	H	N	O
FGS	86.40	4.44	0.00	9.16
FGS-Br[b]	68.70	3.02	2.89	12.97
FGS-PDMAEMA-16 h[c]	62.93	8.35	7.78	19.71

[a] All values are the average of three individual measurements.
[b] The content of Br is estimated to be 12.42%.
[c] Sample from FGS-PDMAEMA-16 h. The content of Br is estimated to be 1.23%.

molecular weight (Supporting Information). Hence, the attachment of FGS with PDMAEMA brushes has a minimal effect on the thermal properties of the attached polymer.

X-ray photoelectron spectroscopy (XPS) studies were employed to monitor the progress of the characteristic binding energy of C1s peaks corresponding to each functional graphene nanosheet (Fig. 3). The deconvoluted high-resolution C1s spectra provided information regarding rich surface functional groups present on the FGS, including sp^2 hybridized graphitic carbons (284.4 eV), sp^3 hybridized saturated carbons (285.0 eV), C–O (285.7 eV), C═O (287.7 eV), and carboxyl groups (290.5 eV), which were all in agreement with previous work. In general, the relative intensities of each peak in XPS varied upon the progress of surface modification. For example, after reacting with surface-initiator group, a new peak attributable to C–Br (285.7 eV) arose while the peak corresponding to sp^2 graphitic carbon (284.5 eV) diminished concomitantly. In addition, this result was further confirmed by the elemental analysis which revealed the presence of Br in the FGS-Br (Table 1). After polymerization via ATRP, observed peaks such as C–O and O═C–O increased sharply which are attributed to covalently attached PDMAEMA. Additionally, the FGS-PDMAEMA still contained a large amount of sp^2 hybridized graphitic carbons (34.6%), albeit at much lower levels compared to pristine FGS (40.5%), which supported the idea that the grafting of PDMAEMA on the surface of graphene sheets does not deteriorate the surface of the graphene nanosheets. Consistent with the XPS data, the Raman spectra displayed characteristic features of chemically functionalized FGS-PDMAEMA, including D (1346 cm^{-1}, disorder due to sp^3 carbon bonds), and G (1596 cm^{-1}, sp^2 stretching in graphitic lattice) (Fig. 4). The relative area ratio of the D to G peaks obtained (I_D/I_G) was also used to provide information of structural defects present in the functionalized FGS [7]. As prepared FSG shows I_D/I_G of 0.94 ± 0.042, and that for FGS-Br was 0.86 ± 0.079. With the progress of polymerization, these values increased to 1.34 ± 0.122 for FGS-PDMAEMA because of the decreased cluster size of sp^2 carbon, consistent with previous studies [44].

The FGS-PDMAEMA suspended in aqueous solution was deposited onto a silicon wafer and subjected to a number of characterizations that clearly demonstrated the functionalized graphene nanosheets. The scanning electron microscopy (SEM) and transmission electron microscopy (TEM) images in Fig. 5 showed the level of exfoliation of dispersed graphene sheets and revealed the presence of thin graphene layers with occasional folding. In clear contrast, as the polymerization proceeded, the functionalized FGS-PDMAEMA displayed thick plates of graphene sheets with dark contrast that are reminiscent of the polymeric structures on the graphene nanosheet.

In an effort to control the dispersion state of these hybrid materials upon temperature change in water, six FGS-PDMAEMA samples with different lengths of PDMAEMA chains were initially

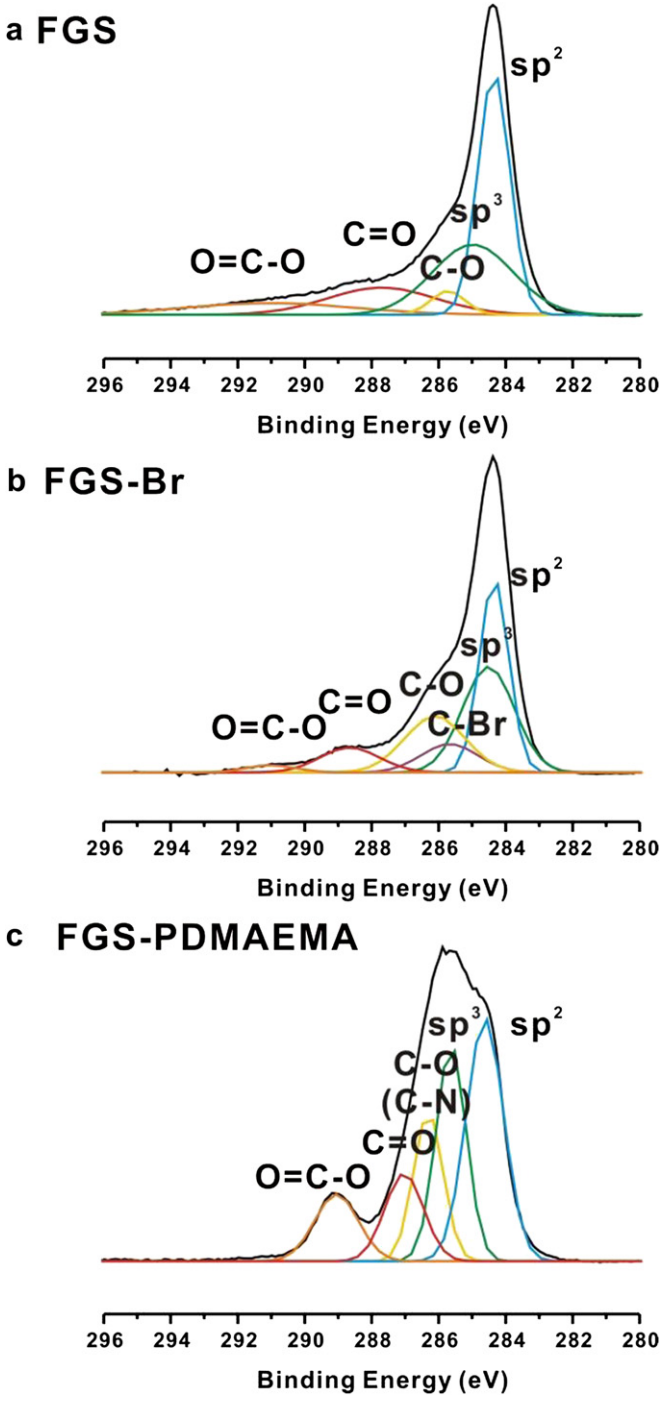

Fig. 3. High-resolution C1s XPS spectra of (a) FGS, (b) FGS-Br, and (c) FGS-PDMAEMA-16 h. The black curves are experimental data with other colored curves for deconvoluted fitting.

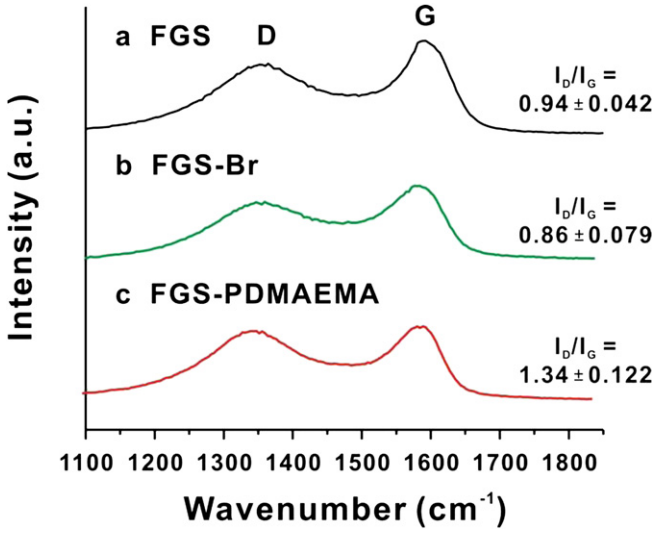

Fig. 4. Raman spectra of (a) FGS, (b) FGS-Br, and (c) FGS-PDMAEMA-16 h with the corresponding I_D/I_G values averaged over five individual samples.

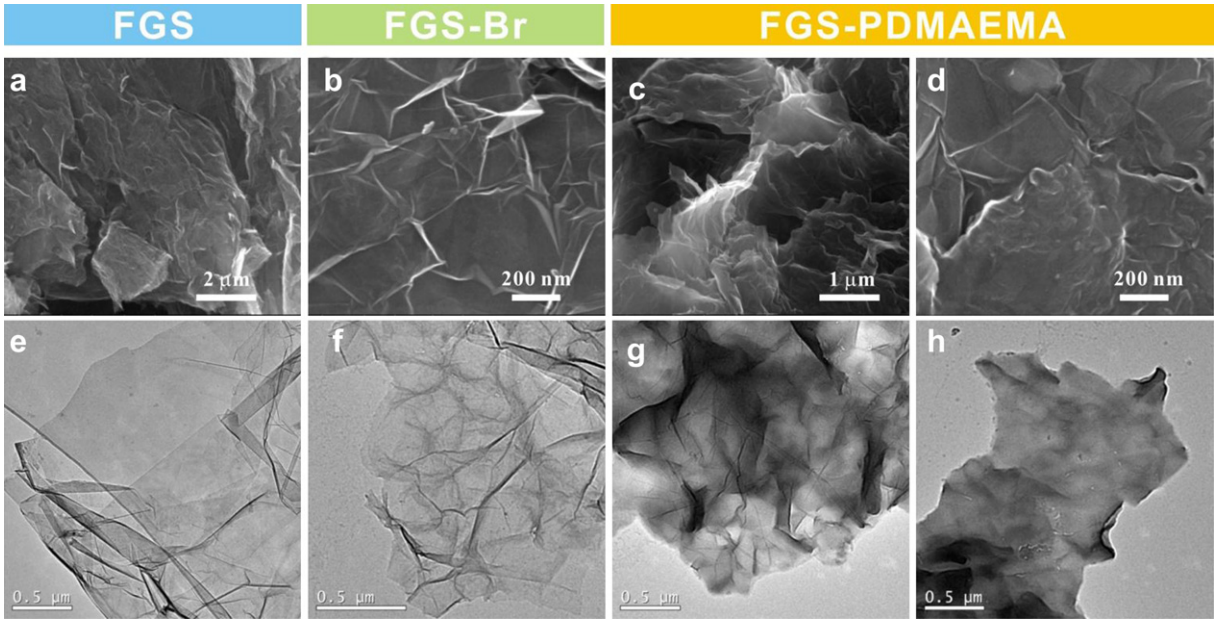

Fig. 5. Representative electron microscopy images of samples prepared in this study. (a–d) SEM and (e–h) TEM images of (a,e) FGS, (b, f) FGS-Br and (c, d, g, h) FGS-PDMAEMA-16 h.

dispersed in water (0.03 wt%). Upon heating, the dispersibility of all FGS-PDMAEMA samples decreased due to the thermoresponsive aggregation of PDMAEMA chains (Fig. 6). It was found that this switching property of the PDMAEMA functionalized FGS was highly dependent on the chain length of polymer, for example, the high molecular weight PDMAEMA (52,000 g/mol) clearly exhibited this phase transfer behavior, while that of PDMAEMA with a low molecular weight range did not display an observable switching property, since the dispersion state of FGSs were not significantly affected by a small fraction of surface grafted PDMAEMA chains.

We then prompted to monitor this interesting aggregation behavior of the PDMAEMA chains upon heating via in situ temperature-dependent ^{1}H NMR measurements of FGS-PDMAEMA-16 h in deuterated water (Supporting Information). The signal at 2.25 ppm is characteristic of a dimethyl group at 25 °C. As the temperature increased to 75 °C, the dimethyl peak not only shifted to higher ppm values, but the peak intensities gradually decreased due to dehydration by disruption of hydrogen bonding with water molecules above the LCST [45].

A unique feature of FGS-PDMAEMA is in that the solubility of FGS can be easily tunable with the temperature changes by exploiting the LCST behavior of the PDMAEMA. As shown in Fig. 7a, an aqueous suspension of FGS-PDMAEMA-16 h was readily transferred into an organic phase upon heating above 60 °C. Then the

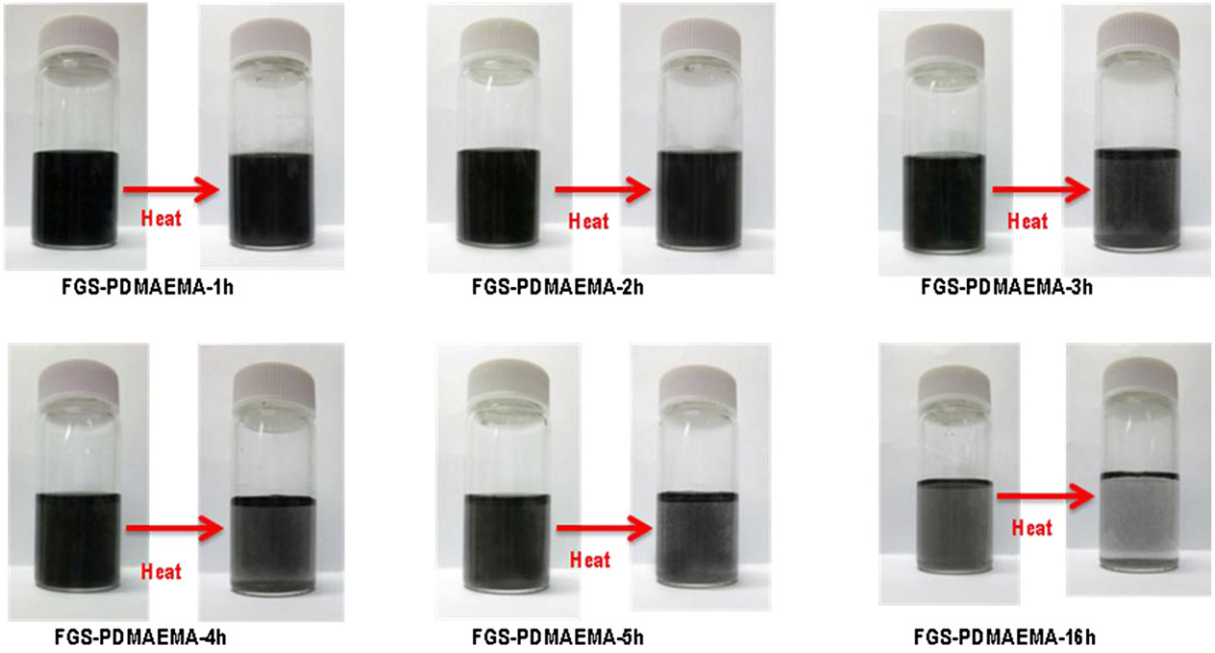

Fig. 6. Photographs of aqueous dispersions of a series of FGS-PDMAEMA samples (left: before heating; right: after heating above 60 °C). All are in the concentration of 0.03 wt%.

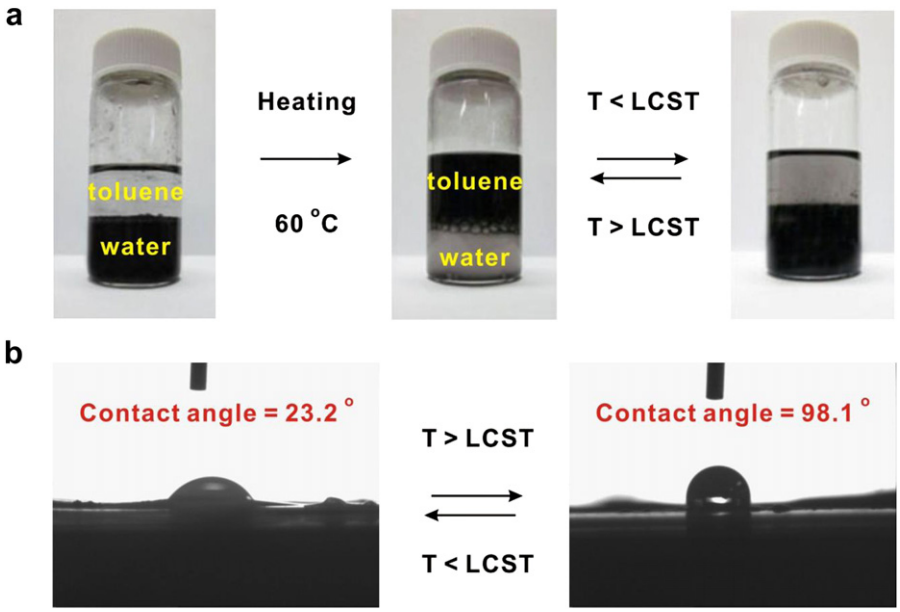

Fig. 7. The thermoresponsive property of FGS-PDMAEMA-16 h (a) the phase transfer of FGS-PDMAEMA-16 h between aqueous and organic phase upon temperature control. (b) contact angle measurement on the film of FGS-PDMAEMA-16 h with heating and cooling cycles.

FGS-PDMAEMA-16 h in an upper toluene phase were transferred back upon cooling down to room temperature. This process was repeated several times without noticing any aggregates. It is also of note that Suh and co-workers have recently demonstrated the reversible phase transfer of graphene sheets between the aqueous and organic phase by the simple anion exchange of ionic liquid modified polymers [46].

In parallel to the solution property of FGS-PDMAEMA, we found that the film of FGS-PDMAEMA sheets displays a similar control over the wettability upon temperature control. The FGS-PDMAEMA sheets suspended in an aqueous solution were deposited onto a silicon wafer to form a homogeneous thin film and then it was subjected to the goniometer to measure the contact angle of water droplet. At room temperature, the contact angle of water droplet was hydrophilic (23.2°), while that changes significantly to hydrophobic (98.1°) upon temperature increase of the sample (Fig. 7b). Taken together, these changes in solubility and wettability of the FGS-PDMAEMA provide direct evidence that the tethered thermoresponsive PDMAEMA brushes can display reversible transitions that are accompanied by measurable changes in the surface property of the graphene nanosheet [47].

4. Conclusions

In summary, FGS-PDMAEMA hybrids were prepared by grafting PDMAEMA chains from the surface of the FGSs. The dispersibility of these composites in water were significantly improved by decorating the FGSs with water-soluble PDMAEMA. The dispersion and aggregation states of these hybrid materials were controlled repetitively upon heating and cooling cycles in water. As the chain length of PDMAEMA increases, this phenomenon becomes more evident. Moreover, the selective dispersion of FGS-PDMAEMA hybrids between aqueous and organic solvent was readily achieved by simple temperature changes. The thin film of the composite was prepared by depositing FGS-PDMAEMA aqueous suspensions on a silicon wafer. Contact angles on composite films were measured before and after heating, and it was demonstrated that the wettability was easily controlled by virtue of the thermoresponsive nature PDMAEMA. The successful dispersion of graphene sheets is anticipated to enable the use of low-cost solution processing techniques to fabricate graphene-based materials and further broaden their applications in graphene-based switching devices and sensors.

Acknowledgments

This work was supported by the Priority Research Center Program (2009-0093818), and Basic Science Research Program (2011-0004822) through the National Research Foundation of Korea funded by the Ministry of Education, Science, and Technology of Korea. This research was also supported by WCU (World Class University) program through the Korea Science and Engineering Foundation funded by the Ministry of Education, Science and Technology (R31-2008-000-20012-0) and by the National Research Foundation of Korea (NRF) grant funded by the Korea government (MEST) (2010-0003219).

Appendix. Supplementary data

Supplementary data related to this article can be found online at doi:10.1016/j.polymer.2011.11.057.

References

[1] Geim AK, Novoselov KS. Nat Mater 2007;6(3):183–91.
[2] Wu J, Pisula W, Muellen K. Chem Rev 2007;107(3):718–47.
[3] Zhang Y, Tan Y-W, Stormer Horst L, Kim P. Nature 2005;438(7065):201–4.
[4] Novoselov KS, Geim AK, Morozov SV, Jiang D, Zhang Y, Dubonos SV, et al. Science 2004;306(5696):666–9.
[5] Li D, Mueller MB, Gilje S, Kaner RB, Wallace GG. Nat Nanotechnol 2008;3(2):101–5.
[6] Park S, An J, Jung I, Piner RD, An SJ, Li X, et al. Nano Lett 2009;9(4):1593–7.
[7] Stankovich S, Dikin DA, Piner RD, Kohlhaas KA, Kleinhammes A, Jia Y, et al. Carbon 2007;45(7):1558–65.
[8] Berger C, Song Z, Li X, Wu X, Brown N, Naud C, et al. Science 2006;312(5777):1191–6.
[9] Sutter PW, Flege J-I, Sutter EA. Nat Mater 2008;7(5):406–11.
[10] Kim Keun S, Zhao Y, Jang H, Lee Sang Y, Kim Jong M, Kim Kwang S, et al. Nature 2009;457(7230):706–10.
[11] Li X, Cai W, Colombo L, Ruoff RS. Nano Lett 2009;9(12):4268–72.
[12] Li X, Zhu Y, Cai W, Borysiak M, Han B, Chen D, et al. Nano Lett 2009;9(12):4359–63.

[13] Schniepp HC, Li J-L, McAllister MJ, Sai H, Herrera-Alonso M, Adamson DH, et al. J Phys Chem B 2006;110(17):8535–9.
[14] McAllister MJ, Li J-L, Adamson DH, Schniepp HC, Abdala AA, Liu J, et al. Chem Mater 2007;19(18):4396–404.
[15] Ramanathan T, Abdala AA, Stankovich S, Dikin DA, Herrera-Alonso M, Piner RD, et al. Nat Nanotechnol 2008;3(6):327–31.
[16] Cai D-Y, Song M. J Mater Chem 2010;20(37):7906–15.
[17] Verdejo R, Bernal MM, Romasanta LJ, Lopez-Manchado MA. J Mater Chem 2011;21(10):3301–10.
[18] Rafiee MA, Rafiee J, Wang Z, Song H, Yu Z-Z, Koratkar N. ACS Nano 2009;3(12): 3884–90.
[19] Yoonessi M, Gaier JR. ACS Nano 2010;4(12):7211–20.
[20] Kim H, Macosko CW. Macromolecules 2008;41(9):3317–27.
[21] Zhang H-B, Zheng W-G, Yan Q, Yang Y, Wang J-W, Lu Z-H, et al. Polymer 2010; 51(5):1191–6.
[22] An X, Simmons T, Shah R, Wolfe C, Lewis KM, Washington M, et al. Nano Lett 2010;10(11):4295–301.
[23] Jo K, Lee T, Choi HJ, Park JH, Lee DJ, Lee DW, et al. Langmuir 2011;27(5): 2014–8.
[24] Feng R, Guan G, Zhou W, Li C, Zhang D, Xiao Y. J Mater Chem 2011;21(11): 3931–9.
[25] Lee YR, Raghu AV, Jeong HM, Kim BK. Macromol Chem Phys 2009;210(15): 1247–54.
[26] Fang M, Wang K, Lu H, Yang Y, Nutt S. J Mater Chem 2009;19(38):7098–105.
[27] Lee SH, Dreyer DR, An J, Velamakanni A, Piner RD, Park S, et al. Macromol Rapid Commun 2010;31(3):281–8.
[28] Goncalves G, Marques PAAP, Barros-Timmons A, Bdkin I, Singh MK, Emami N, et al. J Mater Chem 2010;20(44):9927–34.
[29] Fang M, Wang K, Lu H, Yang Y, Nutt S. J Mater Chem 2010;20(10):1982–92.
[30] Yang Y, Wang J, Zhang J, Liu J, Yang X, Zhao H. Langmuir 2009;25(19): 11808–14.
[31] Wang D, Ye G, Wang X, Wang X. Adv Mater 2011;23(9):1122–5.
[32] Kim H, Abdala A, Macosko CW. Macromolecules 2010;43(16):6515–30.
[33] Wajid AS, Das S, Irin F, Tanvir Ahmed HS, Shelburne JL, Parviz D, Fullerton RJ, Jankowski AF, Hedden RC, and Green MJ. Carbon (0).
[34] Veca LM, Lu F, Meziani MJ, Cao L, Zhang P, Qi G, et al. Chem Commun 2009;(18):2565–7.
[35] Wu W, Tsarevsky NV, Hudson JL, Tour JM, Matyjaszewski K, Kowalewski T. Small 2007;3(10):1803–10.
[36] Lee H-i, Pietrasik J, Sheiko SS, Matyjaszewski K. Prog Polym Sci 2010;35(1–2): 24–44.
[37] Matyjaszewski K, Xia J. Chem Rev 2001;101(9):2921–90.
[38] Wang J-S, Matyjaszewski K. J Am Chem Soc 1995;117(20):5614–5.
[39] Matyjaszewski K, Tsarevsky NV. Nat Chem 2009;1(4):276–88.
[40] Steenackers M, Gigler AM, Zhang N, Deubel F, Seifert M, Hess LH, et al. J Am Chem Soc 2011;133(27):10490–8.
[41] Lee DY, Yoon S, Oh YJ, Park SY, In I. Macromol Chem Phys 2011;212(4): 336–41.
[42] Li GL, Liu G, Li M, Wan D, Neoh KG, Kang ET. J Phys Chem C 2010;114(29): 12742–8.
[43] Kudin KN, Ozbas B, Schniepp HC, Prud'homme RK, Aksay IA, Car R. Nano Lett 2008;8(1):36–41.
[44] Hong T-K, Lee DW, Choi HJ, Shin HS, Kim B-S. ACS Nano 2010;4(7):3861–8.
[45] Jung S-H, Song H-Y, Lee Y, Jeong HM, Lee H-i. Macromolecules 2011;44(6): 1628–34.
[46] Kim T, Lee H, Kim J, Suh KS. ACS Nano 2010;4(3):1612–8.
[47] Jones DM, Smith JR, Huck WTS, Alexander C. Adv Mater 2002;14(16): 1130–4.